JOURNAL OF MATERIALS SCIENCE 23 (1988) 2321–2324

On the constancy of the specific enthalpy of fracture

M. BAKAR, A. CHUDNOVSKY, A. MOET
Department of Macromolecular Science, Case Western Reserve University, Cleveland, Ohio 44106-2699, USA

The specific enthalpy of fracture due to ductile crack propagation in commercial polycarbonate sheet is calculated as $\gamma^* = A_{1c}/R_{1c}$, where A_{1c} is the critical energy release rate associated with the onset of unstable crack propagation and R_{1c} is the corresponding amount of damage (yielded material) formed per unit crack extension. A_{1c} and R_{1c} are determined from fatigue crack propagation experiments conducted at different maximum loads, load ratios and frequencies. The value of γ^* obtained from all experiments is found to be $9.8 \pm 1.4\,\text{cal}\,\text{g}^{-1}$ (1 cal = 4.184 J) which indicates that γ^* is a material constant. This finding substantiates predictions of the crack layer theory.

1. Introduction

The commonly used term '*fracture toughness*' is vaguely defined. Related parameters include the critical stress intensity factor K_{Ic} [1], the critical crack opening displacement δ_c [2], and the critical energy release rate J_{1c} [3]. The first two correspond to spontaneous crack extension. The third, on the other hand, reflects the crack initiation condition. All of them are implied to be material constants. Indeed, for rigidly defined testing procedures, specific values may be obtained repeatedly. Variations in loading conditions and/or specimen configuration, however, lead to significant differences in these values which are proposed to be measures of fracture toughness.

In general, the rate of slow crack propagation plotted as a function of the stress intensity factor or the energy release rate typically displays an S-shaped curve (Fig. 1). At a critical value of K or J_1 a transition form slow to fast (uncontrolled) crack propagation occurs. It would be reasonable to consider these values, i.e., K_{Ic} or J_{1c} as a measure of fracture toughness. Unfortunately, this attractive idea fails the test experiment. It is widely reported that the value of K or J_1 at which the transition from slow to fast crack propagation occurs varies significantly with loading history.

In the crack layer theory [4–6], which accounts for the damage accompanying crack propagation, fracture toughness is introduced through conditions of crack layer instability, i.e.,

$$J_1 - \gamma^* R_1 = 0 \tag{1}$$

and

$$\frac{\partial}{\partial l}(J_1 - \gamma^* R_1) > 0 \tag{2}$$

where γ^* is the specific enthalpy of damage, l is the crack length, and R_1 is an intergral characteristic of damage formation associated with crack advance. The theory introduces γ^* as a material constant, and the resistance moment R_1 as a history dependent parameter.

This paper presents results of an experiment designed to test the constancy of γ^* for different loading conditions. Thin polycarbonate sheet has been chosen as a model material since the damage associated with crack propagation appears as *homogeneous* material transformation (yielding). Single-edge notched (SEN) specimen geometry has been employed because condition 2 expressed above is met prior to 1 and thus 1 becomes a necessary and sufficient condition of instability.

2. Experimental procedure

SEN specimens ($20 \times 80\,\text{mm}^2$) are milled from a 6 mm thick, extruded sheet of bisphenol-A polycarbonate, whose density is $1.208\,\text{g}\,\text{cm}^{-3}$. The sheets are obtained from Transilwrap Corporation (Cleveland, Ohio). A straight notch of 1 mm depth is introduced with a razor blade attached to the crosshead of an Instron machine, at a constant rate of penetration ($5\,\text{mm}\,\text{min}^{-1}$). Fatigue crack propagation tests are conducted on an MTS-800 machine using a sinusoidal wave form at constant frequencies of 0.01, 0.1 and 1.0 Hz. The loading is carried out in tension–tension with different maximum applied stresses (30, 35, 40, and 48 MPa), and load ratios of 0.1, 0.3 and 0.5. Crack growth and evolution of the surrounding damage zone are observed by means of a travelling optical microscope attached to a video camera assembly. Concurrently, load–displacement curves are recorded by means of an x–y chart recorder. Crack propagation and crack layer evolution were measured from video playbacks.

3. Results and discussion

3.1. Mechanism of crack layer propagation

Fig. 2a is a transmitted light micrograph of a crack surrounded by transformed material, i.e., a crack

0022–2461/88 $03.00 + .12

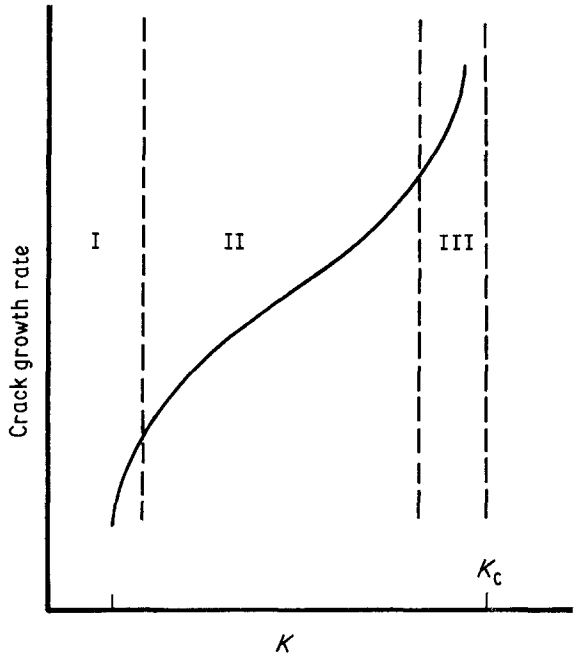

Figure 1 A schematic for crack propagation kinetics showing its three stages.

Figure 3 A reflected light micrograph of a section normal to crack propagation plane showing yielding profile of the active zone.

layer. The dark contour indicates the boundary of the transformed (yielded) material. The sketch in Fig. 2b shows a three dimensional view of half of the specimen after fracture. Obviously, the size of the transformed zone evolves with crack growth. This type of transformation is observed for all loading conditions considered in the study. However, the size of the transformed zone varies with loading condition [7].

The extent of yielding is examined through a cross-section normal to the direction of crack propagation. A typical micrograph of such a cross-section is exhibited in Fig. 3. It shows constant material thinning (yielding) within the layer and a relatively small transitional zone at its boundary with the initial material.

To examine the nature of the material transformation, density measurements [8] were carried out. It was found that the density of the transformed material increased to $1.213\,g\,cm^{-3}$ from an initial value of $1.208\,g\,cm^{-3}$. This change is independent of the applied loading condition which suggests that the transformation associated with crack propagation is unaltered by loading.

3.2. Energy release rate evaluation

Since the active zone (Fig. 2a) is relatively large with respect to the crack length and the width of the specimen for a crack approaching instability, elastic solution of the energy release rate is no longer applicable. Known elastoplastic solutions are not applicable either since they predict plastic zone shape and size essentially different from the zone observed. Therefore, the energy release rate was evaluated experimentally using conventional techniques based on evolution of the load–displacement curves [9].

Fig. 4 shows the experimentally measured energy release rate for a crack propagating under σ_{max} =

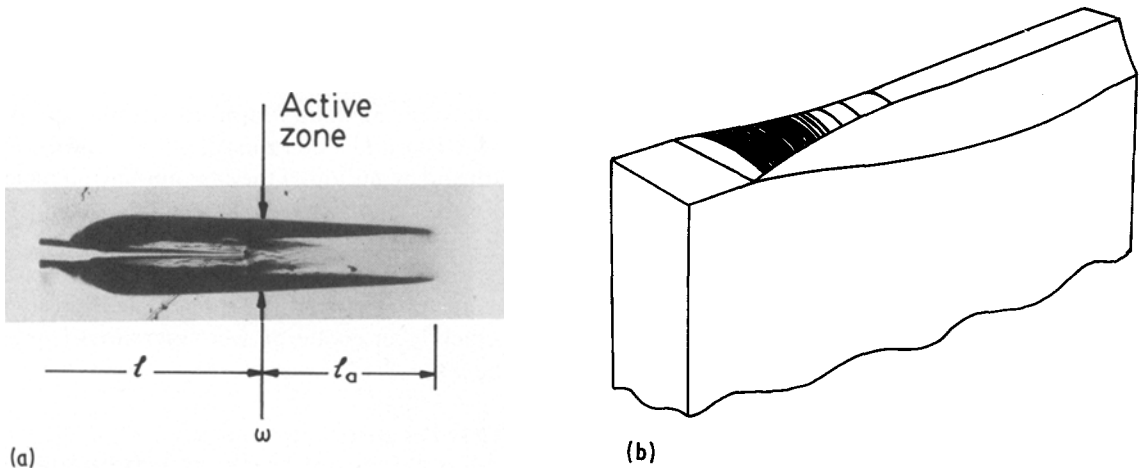

Figure 2 (a) Transmitted light micrograph of a crack layer in 0.25 mm thin polycarbonate sheet. (b) A sketch of one-half of the fractured specimen illustrating damage evolution (yielding of the material).

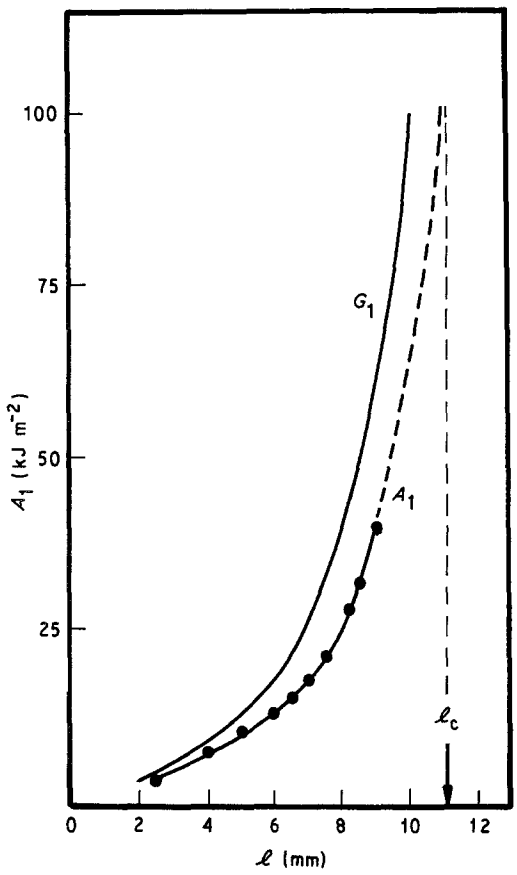

Figure 4 Comparison between the measured total energy release rate (A_1) and the calculated energy release rate (G_1) as a function of crack length for $\sigma_{max} = 30\,MN\,m^{-2}$ at a frequency of 0.1 Hz and a load ratio of 0.1.

30 MN m^{-2}. The elastic solution with Irwin correction for the plastic zone G_1 is also presented for comparison. The theoretical curve obviously overestimates the energy release rate, although qualitatively it resembles the experimentally obtained data. This qualitative agreement justifies extrapolation to assess the critical energy release rate value. Fourth-order polynomial fit was determined to be appropriate for this task.

It should be noted that the measured energy release rate contains the energy released due to active zone translation which coincides with J_1, and the energy released due to active zone deformation. Thus, to distinguish between the total energy release rate and the conventionally used translational energy release rate J_1, we assign the former as A_1 [6].

Table I summarizes values of A_{1c} for different loading conditions. Obviously, the critical energy release rate varies more than a factor of three for an approximately 60% increase in σ_{max}. Thus, such a parameter may not be considered as a material parameter.

TABLE I Total critical energy release rate (A_{1c}) experimentally evaluated at different loading conditions

σ_{max} (MPa)	30	35	40	48		30			30	
$\sigma_{min}/\sigma_{max}$		0.1			0.1	0.3	0.5		0.1	
Frequency (Hz)		0.1				0.1		1.0	0.1	0.01
A_1 (kJ m^{-2})	101	166	229	351	101	102	105	110	101	194

3.3. Evaluation of resistance moment

In general, the resistance moment R_1 is defined as the amount of damage formed per unit crack extension [4]. In cases where the damage species encountered are discrete discontinuities, such as microcracks, its density ϱ is readily measured as the area of middle crack plane per unit volume. When damage consists of crazes, a similar measure of ϱ can be introduced as the area of middle craze plane per unit volume [10, 11]. R_1 is expressed by the following integral over the trailing edge of the active zone $\Gamma^{(t)}$:

$$R_1 = \int_{\Gamma^{(t)}} \varrho n_1 \, d\Gamma \qquad (3)$$

where n_1 is the projection of the unit normal vector on the tangent to the crack trajectory at the crack tip [4]. Thus, for the case in which active zone damage consists of microcracks, R_1 is expressed as the amount of microcrack surfaces per unit crack extension (m^2 m^{-2}). The corresponding energy release rate units are J m^{-2}. Of course, knowledge of the volume fraction of the fibrillar material within the craze and its average opening enables the conversion of the dimensionality of R_1 into volume of transformed material per unit crack extension (m^3 m^{-2}) [11]. Consequently, the corresponding energy units are J m^{-3}.

In the present case, "damage", i.e., material transformation within the active zone, consists of homogeneous yielding. Thus, R_1 can be measured simply as the volume of transformed material per unit crack extension. In view of the fact that yielding is practically uniform over the entire crack layer width (Fig. 3), the volume of transformed material was calculated from the areal increment of the side view of the active zone (Fig. 2a) and the thickness of the layer measured from the fracture surface (Fig. 2b). Subsequent to an initial stage of non-linearity, R_1 increased linearly with crack length. An example of this behaviour under different maximum stress levels is shown in Fig. 5.

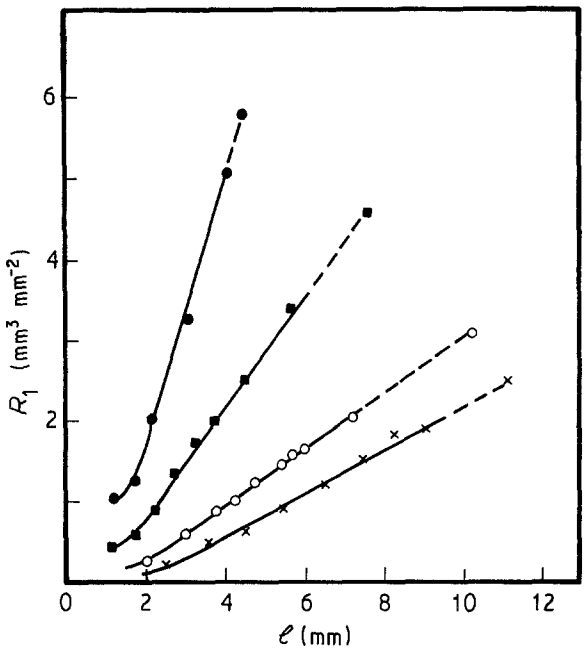

Figure 5 Evolution of the crack layer resistance moment (R_1) under different stress levels at (● 48 MPa, ■ 40 MPa, ○ 35 MPa, x 30 MPa) at a frequency of 0.1 Hz and load ratio of 0.1.

TABLE II Total critical resistance moment (R_{Ic}) experimentally evaluated at different loading conditions

σ_{max} (MPa)	30	35	40	48	30			30		
$\sigma_{min}/\sigma_{max}$		0.1			0.1	0.3	0.5	0.1		
Frequency		0.1				0.1		1.0	0.1	0.01
R_I ($mm^3\,m^{-2}$)	2.4	3.1	4.6	5.8	2.4	1.9	2.0	2.4	2.4	3.5

TABLE III The specific enthalpy of damage (yielding) calculated as $\gamma^* = A_{Ic}/R_{Ic}$

σ_{max} (MPa)	30	35	40	48	30			30		
$\sigma_{min}/\sigma_{max}$		0.1			0.1	0.3	0.5	0.1		
Frequency		0.1				0.1		1.0	0.1	0.01
γ^* ($cal\,g^{-1}$)	8.3	10.6	9.8	11.8	8.3	10.6	10.3	9.1	8.3	10.9

Observed linearity of the $R_I - l$ relationship permits evaluation of R_{Ic} by simple extrapolation. Table II summarizes the critical values of R_{Ic} for all loading conditions. Within this range of loading conditions, R_{Ic} varies roughly by a factor of three.

3.4. Specific enthalpy of damage

As alluded to earlier in the introduction, crack layer propagation in SEN specimen under fixed sinusoidal loads satisfies condition 2 of instability prior to condition 1. Accordingly, the specific enthalpy of damage (yielding in the present case) can be evaluated from conditon 1, i.e., $\gamma^* = A_{Ic}/R_{Ic}$ ($J\,m^{-3}$). The date in Tables I and II are used for this calculation. In view of the fact that specific enthalpy is usually reported in calories per unit mass, the units $J\,m^{-3}$ is converted to $cal\,g^{-1}$ ($1\,cal = 4.184\,J$) employing the measured density of transformed material ($1.213\,g\,cm^{-3}$). Results of these calculations are shown in Table III. The average specific enthalpy of damage is $9.8\,cal\,g^{-1}$ with a standard deviation of $1.4\,cal\,g^{-1}$. Fluctuation of the reported values lies within reasonable range of the expected experimental errors.

4. Concluding remarks

The results demonstrate that the critical energy release rate associated with the transition from slow to fast (uncontrolled) crack propagation varies significantly and cannot be considered as a material parameter. Dependence of the resistance moment upon loading conditions is basically responsible for the noted variations in the critical energy relase rate. At the same time, the specific enthalpy of damage is practically constant. Accordingly, the fracture toughness of a material can be completely characterized by the specific enthalpy of damage and an equation for the resistance moment evolution in terms of loading history. A thermodynamic argument to construct such a constitutive equation has been recently presented [6]. It should be emphasized that fracture toughness should be characterized by a material constant which would reflect the failure mechanism together with an equation describing the response of material to stress level and rate of stress application.

Acknowledgements

Financial support of Dow Chemical Company for our research on polycarbonate fracture is gratefully appreciated. The authors are also grateful for useful discussions with Dr R. Bubek and Dr C. Bosnyak, and for the assistance of M. Napolitano with density measurements.

References

1. ASTM Standard E399-78A, Annual Book of ASTM Standards, Part 10 (1979) p. 540.
2. British Standard Institution BS5762, BSI London (1979).
3. ASTM Standard E813-81, Annual Book of ASTM Standards, (1982) p. 822.
4. A. CHUDNOVSKY and A. MOET, *J. Mater. Sci.* **20** (1985) 630.
5. *Idem, Elastomers Plastics* **18** (1986) 50.
6. A. CHUDNOVSKY, *J. Appl. Mech.* (ASME), in press.
7. M. BAKAR, PhD. Thesis, Case Western Reserve University (1986).
8. G. C. IVES, J. A. MEAD and M. M. RILEY, "Handbook of Plastics Testing Methods", (Illiffe Books, London, 1971) p. 78.
9. N. HADDAOUI, A. CHUDNOVSKY and A. MOET, *Polymer* **27** (1986) 1377.
10. A. CHUDNOVSKY, A. MOET, R. J. BANKERT and M. T. TAKEMORI, *J. Appl. Phys.* **54** (1983) 5562.
11. J. BOTSIS, A. CHUDNOVSKY and A. MOET, *Int. J. Fracture* **33** (1987) 277.

Received 8 October
and accepted 16 December 1987